

DESY 06-237  
KEK-TH-1124  
KIAS-P06063  
December 19, 2006

## $\tau$ Polarization in SUSY Cascade Decays

S.Y. Choi<sup>1,2</sup>, K. Hagiwara<sup>3</sup>, Y.G. Kim<sup>4</sup>, K. Mawatari<sup>5</sup> and P.M. Zerwas<sup>2,3</sup>

<sup>1</sup> *Physics Department and RIPC, Chonbuk University, Jeonju 561-756, Korea*

<sup>2</sup> *Deutsches Elektronen-Synchrotron DESY, D-22603 Hamburg, Germany*

<sup>3</sup> *Theory Division, KEK, Tsukuba, Ibaraki 305-0801, Japan*

<sup>4</sup> *ARCSEC, Sejong University, Seoul 143-747, Korea*

<sup>5</sup> *School of Physics, Korea Institute for Advanced Study, Seoul 130-722, Korea*

### Abstract

$\tau$  leptons emitted in cascade decays of supersymmetric particles are polarized. The polarization may be exploited to determine spin and mixing properties of the neutralinos and stau particles involved.

1.) A rich source of information on supersymmetric particles and the structure of the underlying theory can eventually be provided at LHC [1, 2] by cascade decays. After squarks and gluinos are copiously produced in high energy proton-proton collisions [3], they cascade down, generally in several steps, to the lightest supersymmetric particle, thereby generating intermediate non-colored supersymmetric states like charginos/neutralinos and sleptons [4] which are difficult to produce otherwise at a hadron collider.

Much attention has been paid in the recent past to the SPS1a cascade [5]

$$\tilde{q} \rightarrow q\tilde{\chi}_2^0 \rightarrow q\ell\tilde{\ell} \rightarrow q\ell\ell\tilde{\chi}_1^0 \quad (1)$$

which gives rise to a well-populated ensemble of neutralinos and  $R$ -type sleptons with ratios of 30%, 10% and 100% in the first, second and third branching, respectively. Analyzing the visible  $q\ell\ell$  final state in various combinations of leptons and quark jet, the cascade has served to study the precision with which the masses of supersymmetric particles can be measured at LHC, for a summary see Ref. [6]. In addition, invariant mass distributions have been shown sensitive to the spin of the particles involved [7–10], shedding light on the very nature of the new particles observed in the cascade and on the underlying physics scenario.

So far, cascades have primarily been studied involving first and second generation leptons/sleptons. In this brief note we will explore how the polarization of  $\tau$  leptons can be exploited to study  $R/L$  chirality and mixing effects in both the  $\tilde{\tau}$  and the neutralino sectors.\* As expected, it turns out that measuring the correlation of the  $\tau$  polarizations provides an excellent instrument to analyze these effects.

As polarization analyzer we will use single pion decays of the  $\tau$ 's. At high energies the mass of the  $\tau$  leptons can be neglected and the fragmentation functions are linear in the fraction  $z$  of the energy transferred from the polarized  $\tau$ 's to the  $\pi$ 's [12]:

$$(\tau_R)^\pm \rightarrow \nu_\tau^{(-)} \pi^\pm : F_R = 2z \quad (2)$$

$$(\tau_L)^\pm \rightarrow \nu_\tau^{(-)} \pi^\pm : F_L = 2(1-z) \quad (3)$$

In the relativistic limit, helicity and chirality are of equal and opposite sign for  $\tau^-$  leptons and  $\tau^+$  anti-leptons, respectively. For notational convenience we characterize the  $\tau$  states by chirality.

This note should serve only as an exploratory theoretical study. Experimental simulations will include other  $\tau$  decay final states in addition to pions, *e.g.*  $\rho$ 's and  $a_1$ 's. The  $\rho$ -meson mode is expected to contribute to the  $\tau$ -spin correlation measurement even if the  $\pi^\pm$  and  $\pi^0$  energies are not measured separately. In this case the  $\tau$  polarization analysis power of the  $\rho$  channel is  $\kappa_\rho = (m_\tau^2 - 2m_\rho^2)/(m_\tau^2 +$

---

\*For a discussion of polarization effects in single  $\tau$  decays see Ref. [11].

$2m_\rho^2) \sim 1/2$  in contrast to  $\kappa_\pi = 1$ , but its larger branching fraction of  $B_\rho \approx 0.25$ , versus  $B_\pi \approx 0.11$ , more than compensates for the reduced analysis power. Moreover, in actual experiments it should be possible to measure the  $\pi^\pm$  energy and the  $\gamma$  energies of the  $\pi^0$ 's, all emitted along the parent  $\tau$ -momentum direction at high energies. Significant improvement of the  $\tau$  analysis power is therefore expected from the  $\rho$  and  $a_1$  modes by determining the momentum fraction of  $\pi^\pm$  in the collinear limit of their decays [12]. For each mode, cuts and efficiencies for  $\tau$  identification must be included to arrive finally at realistic error estimates. The large size of the polarization effects predicted on the theoretical basis, and exemplified quantitatively by the pion channel, should guarantee their survival in realistic experimental environments, and we expect that they can be exploited experimentally in practice.

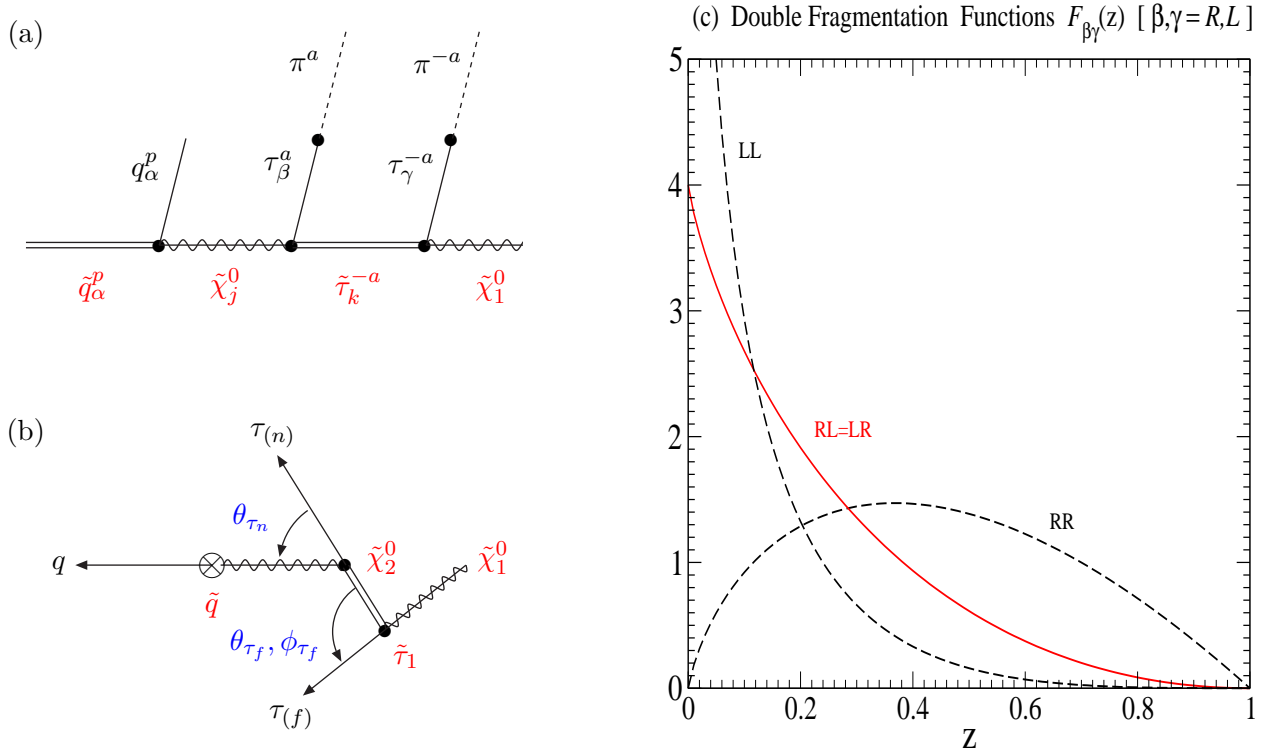


**Figure 1:** (a) The general structure of the quantum numbers of the particles involved in the cascade (1); (b) the angular configuration of the particles in the squark/ $\tilde{\chi}_2^0/\tilde{\tau}_1$  rest frames; and (c) the spectrum of the double  $\tau_\beta\tau_\gamma \rightarrow \pi\pi$  fragmentation functions  $F_{\beta\gamma}$  ( $\beta, \gamma = R, L$ ) with  $z = m_{\pi\pi}^2/m_{\tau\tau}^2$ .

2.) The distribution of the visible final state particles in the squark cascade can be cast, for massless quark  $q$  and no squark  $\tilde{q}$  mixing, in the general form [8]:

$$\frac{1}{\Gamma_{\tilde{q}_\alpha}} \frac{d\Gamma_{\alpha\beta\gamma}^{pa;jk}}{d\cos\theta_{\tau_n} d\cos\theta_{\tau_f} d\phi_{\tau_f}} = \frac{1}{8\pi} \text{B}(\tilde{q}_\alpha \rightarrow q_\alpha \tilde{\chi}_j^0) \text{B}(\tilde{\chi}_j^0 \rightarrow \tau_\beta \tilde{\tau}_k) \text{B}(\tilde{\tau}_k \rightarrow \tau_\gamma \tilde{\chi}_1^0) [1 + (pa)(\alpha\beta) \cos\theta_{\tau_n}] \quad (4)$$

with  $j = 2$  and  $k = 1$  for the squark chain of Eq. (1). The structure of the quantum numbers in the cascade is depicted in Fig. 1(a) while the configuration of the particles in the squark/ $\tilde{\chi}_2^0/\tilde{\tau}_1$  rest frames is shown in Fig. 1(b). For clarity the definitions are summarized in the following table:

$p = \pm :$	particle/anti-particle	$\alpha = \pm :$	$\tilde{q}$ and $q$ $R/L$ chirality
$a = \pm :$	$\tau$ and $\pi$ charge	$\beta = \pm :$	near $\tau_n$ $R/L$ chirality
$j = 2, 3, 4 :$	neutralino mass index	$\gamma = \pm :$	far $\tau_f$ $R/L$ chirality
$k = 1, 2 :$	$\tilde{\tau}$ mass index		

(5)

Near ( $n$ ) and far ( $f$ ) indices denote  $\tau$  and  $\pi$  particles emitted in  $\tilde{\chi}_j^0$  and  $\tilde{\tau}_k$  decays, respectively.

The quark/squark/neutralino  $q_\alpha \tilde{q}_\alpha \tilde{\chi}_j^0$  and the tau/stau/neutralino  $\tau_\beta \tilde{\tau}_k \tilde{\chi}_j^0$  vertices are given by the proper current couplings and the neutralino and stau mixing matrix elements,

$$\langle \tilde{\chi}_j^0 | \tilde{q}_\alpha | f_\alpha \rangle = ig A_{\alpha\alpha j}^q \quad \text{and} \quad \langle \tilde{\chi}_j^0 | \tilde{\tau}_k | \tau_\beta \rangle = ig A_{\beta k j}^\tau \quad [\gamma \text{ correspondingly}] \quad (6)$$

with the explicit form of the couplings  $A_{\alpha\alpha j}^q$  and  $A_{Rkj}^\tau/A_{Lkj}^\tau$

$$A_{LLj}^q = -\sqrt{2}[T_3^q N_{j2}^* + (e_q - T_3^q) N_{j1}^* t_W] \quad (7)$$

$$A_{RRj}^q = +\sqrt{2}e_q N_{j1} t_W \quad (8)$$

$$A_{Lkj}^\tau = -h_\tau N_{j3}^* U_{\tilde{\tau}_k 2} + \frac{1}{\sqrt{2}}(N_{j2}^* + N_{j1}^* t_W) U_{\tilde{\tau}_k 1} \quad (9)$$

$$A_{Rkj}^\tau = -h_\tau N_{j3} U_{\tilde{\tau}_k 1} - \sqrt{2} N_{j1} t_W U_{\tilde{\tau}_k 2} \quad (10)$$

in terms of the  $4 \times 4$  neutralino mixing matrix  $N$  in the standard gaugino/higgsino basis [13] and the  $2 \times 2$  stau mixing matrix  $U_{\tilde{\tau}}$  in the  $L/R$  basis [14]. Here,  $T_3^q = \pm 1/2$  and  $e_q = 2/3, -1/3$  are the  $SU(2)$  doublet quark isospin and electric charge,  $t_W = \tan\theta_W$  and  $h_\tau = m_\tau/\sqrt{2}m_W \cos\beta$ . The distribution (4) depends only on the ‘‘near  $\tau$ ’’ angle  $\theta_{\tau_n}$ ; this is a consequence of the scalar character of the intermediate stau state that erases all angular correlations.

The angles in the cascade Fig. 1(b) are related to the invariant masses [9],

$$m_{\tau\tau}^2 = \frac{1}{2}(1 - \cos\theta_{\tau_f}) \quad \max M_{\tau\tau}^2 = m_{\tilde{\chi}_j^0}^2(1 - m_{\tilde{\tau}_k}^2/m_{\tilde{\chi}_j^0}^2)(1 - m_{\tilde{\chi}_1^0}^2/m_{\tilde{\tau}_k}^2) \quad (11)$$

$$m_{q\tau_n}^2 = \frac{1}{2}(1 - \cos\theta_{\tau_n}) \quad \max M_{q\tau_n}^2 = m_{\tilde{q}_\alpha}^2(1 - m_{\tilde{\chi}_j^0}^2/m_{\tilde{q}_\alpha}^2)(1 - m_{\tilde{\tau}_k}^2/m_{\tilde{\chi}_j^0}^2) \quad (12)$$

$$m_{q\tau_f}^2 = \frac{1}{4}(1 + c_n)(1 - c_f) - \frac{r_{jk}}{2} s_n s_f \cos\phi_{\tau_f} \quad \max M_{q\tau_f}^2 = m_{\tilde{q}_\alpha}^2(1 - m_{\tilde{\chi}_j^0}^2/m_{\tilde{q}_\alpha}^2)(1 - m_{\tilde{\chi}_1^0}^2/m_{\tilde{\tau}_k}^2) \quad (13)$$

$$+ \frac{r_{jk}^2}{4}(1 - c_n)(1 + c_f)$$

where  $r_{jk} = m_{\tilde{\tau}_k}/m_{\tilde{\chi}_j^0}$  and abbreviations  $c_n = \cos \theta_{\tau_n}$ ,  $c_f = \cos \theta_{\tau_f}$  etc are introduced. It proves useful to define the invariant masses,  $m_{\tau\tau}^2$ ,  $m_{q\tau_n}^2$  and  $m_{q\tau_f}^2$ , in units of their maximum values,  $\max M_{\tau\tau}^2$ ,  $\max M_{q\tau_n}^2$  and  $\max M_{q\tau_f}^2$ ; the invariant masses  $m_{\pi\pi}^2$  etc are scaled analogously.

Pion distributions, summed over near and far particles, are predicted by folding the original single  $\tau$  and double  $\tau\tau$  distributions,  $d\Gamma_\beta/dm_{q\tau}^2$  and  $d\Gamma_{\beta\gamma}/dm_{\tau\tau}^2$ , with the single and double fragmentation functions  $F_\beta$  and  $F_{\beta\gamma}$ , where the indices  $\beta, \gamma$  denote the chirality indices  $R/L$  of the  $\tau$  leptons. Based on standard techniques, the following relations can easily be derived for  $[q\pi]$  and  $[\pi\pi]$  distributions:

$$\frac{d\Gamma}{dm_{q\pi}^2} = \int_{m_{q\pi}^2}^1 \frac{dm_{q\tau}^2}{m_{q\tau}^2} \frac{d\Gamma_\beta}{dm_{q\tau}^2} F_\beta \left( \frac{m_{q\pi}^2}{m_{q\tau}^2} \right) \quad (14)$$

$$\frac{d\Gamma}{dm_{\pi\pi}^2} = \int_{m_{\pi\pi}^2}^1 \frac{dm_{\tau\tau}^2}{m_{\tau\tau}^2} \frac{d\Gamma_{\beta\gamma}}{dm_{\tau\tau}^2} F_{\beta\gamma} \left( \frac{m_{\pi\pi}^2}{m_{\tau\tau}^2} \right) \quad (15)$$

The single and double distributions  $d\Gamma_\beta/dm_{q\tau}^2$  and  $d\Gamma_{\beta\gamma}/dm_{\tau\tau}^2$ , can be derived from Eq.(4) by integration. The single  $\tau_\beta \rightarrow \pi$  fragmentation function, *cf.* Eqs.(2) and (3) with  $z = m_{q\pi}^2/m_{q\tau}^2$ , can be summarized as

$$F_\beta(z) = 1 + \beta(2z - 1) \quad (16)$$

while the double  $\tau_\beta\tau_\gamma \rightarrow \pi\pi$  fragmentation functions, with  $z = m_{\pi\pi}^2/m_{\tau\tau}^2$ , are given by

$$F_{RR}(z) = 4z \log \frac{1}{z} \quad (17)$$

$$F_{RL}(z) = F_{LR}(z) = 4 \left[ 1 - z - z \log \frac{1}{z} \right] \quad (18)$$

$$F_{LL}(z) = 4 \left[ (1+z) \log \frac{1}{z} + 2z - 2 \right] \quad (19)$$

The shape of the distributions  $F_{\beta\gamma}(z)$  ( $\beta, \gamma = R, L$ ) is presented in Fig. 1(c). All distributions, normalized to unity, are finite except  $F_{LL}$  which is logarithmically divergent for  $z \rightarrow 0$ .

The great potential of polarization measurements for determining spin and mixing phenomena is demonstrated in Figs. 2(a/b), displaying the invariant mass distribution of (a)  $\tau\tau$  and (b)  $\pi\pi$  pairings in the  $\tilde{\chi}_2^0$  decays of the cascade (1). While the lepton-lepton invariant mass does not depend on the chirality indices of the near and far tau leptons  $\tau_n$  and  $\tau_f$ , the shape of the pion distribution depends strongly on the indices, as expected. This is also reflected in the expectation values of the invariant masses:

$$\langle m_{\pi\pi}^2 \rangle = \begin{cases} 4/18 \\ 2/18 \\ 1/18 \end{cases} \quad \text{and} \quad \langle m_{\tau\tau}^2 \rangle = \begin{cases} 288/675 & \text{for } RR \\ 192/675 & \text{for } RL/LR \\ 128/675 & \text{for } LL \end{cases} \quad (20)$$

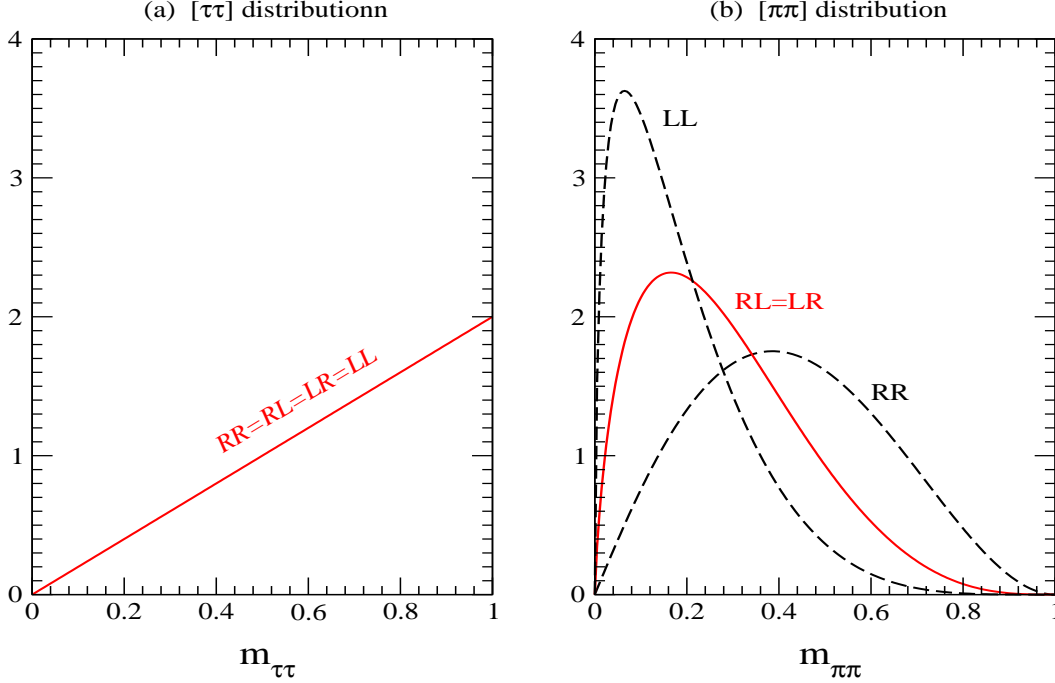


**Figure 2:** The “normalized” invariant mass distributions of (a)  $\tau\tau$  and (b)  $\pi\pi$  pairings in the  $\tilde{\chi}_2^0$  decays of the cascade (1). The indices denote the chiralities of the near and far tau leptons.

which are distinctly different for the pion final states. Due to the scalar stau intermediate state, the  $\tau\tau$  and  $\pi\pi$  distributions do not depend on the polarization state of the parent  $\tilde{\chi}_2^0$  state [contrary to the  $q\tau$  and  $q\pi$  distributions in the chain].

Cutting out small transverse pion momenta in actual experiments will modify the distributions of the  $\pi\pi$  invariant mass, and the distributions are shifted to larger  $m_{\pi\pi}$  values. For  $R$  chiralities of the  $\tau$ 's, with hard  $\tau \rightarrow \pi$  fragmentation, the shift is smaller than for  $L$  chiralities with soft fragmentation. [This will be analyzed quantitatively in the next section for the specific reference point SPS1a.]

**3.)** The sensitivity of various distributions  $[\tau\tau]$ ,  $[q\tau^+]$ ,  $[q\tau^-]$  and  $[\pi\pi]$ ,  $[q\pi^+]$ ,  $[q\pi^-]$  in the cascade (1) starting with a left-handed squark  $\tilde{q}_L$  is studied in the tableau of Fig. 3. The distributions are compared for the SUSY chain in SPS1a, in which the probability for  $\tilde{\tau}_R$  in  $\tilde{\tau}_1$  is close to 90%, with a spin chain (UED') characteristic for universal extra-dimension models [15, 16]:

$$q_1 \rightarrow qZ_1 \rightarrow q\ell\ell_1 \rightarrow q\ell\ell\gamma_1 \quad (21)$$

To focus on the spin aspects,<sup>†</sup> the same mass spectrum is chosen in the UED' as in the SUSY chain:  $m_{\tilde{q}_L} = m_{q_1} = 570.6$  GeV,  $m_{\tilde{\chi}_2^0} = m_{Z_1} = 176.4$  GeV,  $m_{\tilde{\tau}_1} = m_{\tau_1} = 134.1$  GeV and  $m_{\tilde{\chi}_1^0} = m_{\gamma_1} = 98.6$

<sup>†</sup>For this purpose we deliberately ignore the naturally expected mass pattern in models of universal extra dimensions.

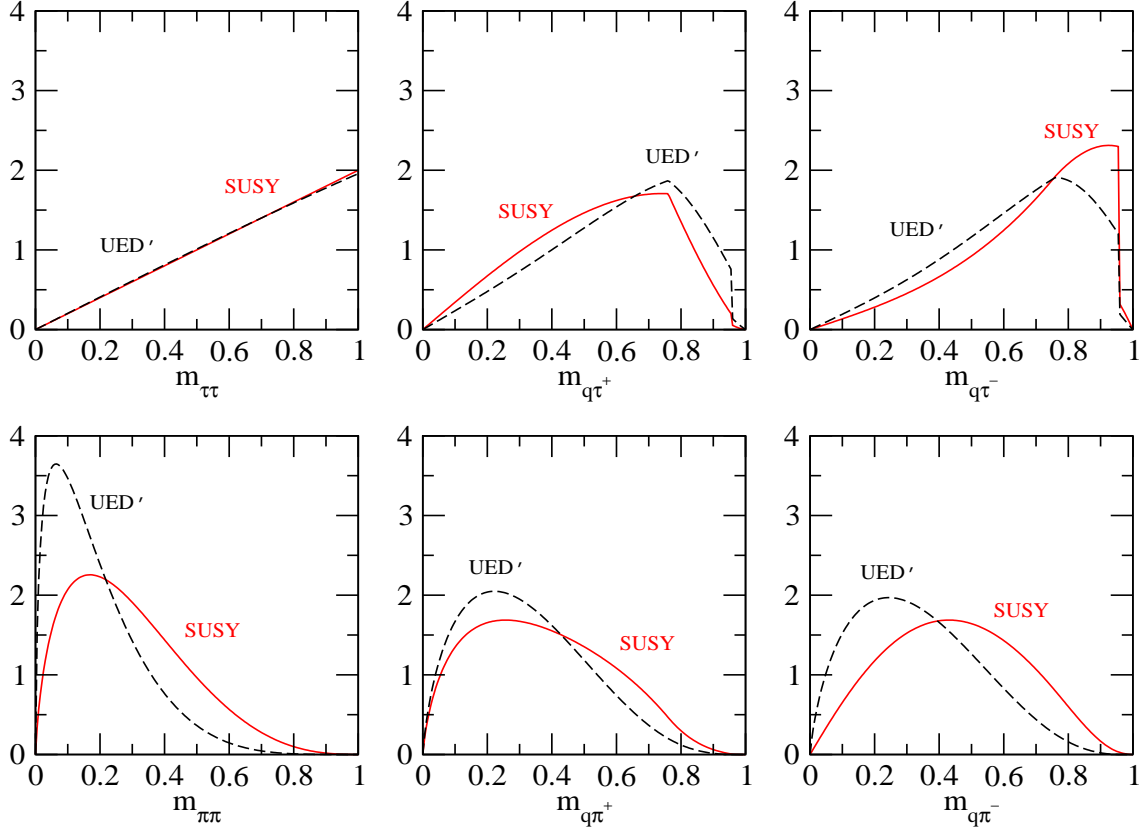


**Figure 3:** The “normalized” distributions in supersymmetry and  $UED'$  for the particle spectrum corresponding to the SUSY scenario  $SPS1a$ ; the distributions  $[\tau\tau]$ ,  $[q\tau^+]$  and  $[q\tau^-]$  in the upper frames and the distributions  $[\pi\pi]$ ,  $[q\pi^+]$  and  $[q\pi^-]$  in the lower frames.

GeV. The  $[\tau\tau]$  distribution is linear  $\sim m_{\tau\tau}$  in supersymmetry. It deviates slightly from the linear dependence in the  $\tau\tau$  invariant mass in  $UED'$  where in the limit of degenerate KK masses the distribution reads  $\sim m_{\tau\tau}[1 - \frac{1}{5}m_{\tau\tau}^2]$ . The kinks in the invariant mass distributions  $[q\tau]$  and  $[q\pi]$  signal the transition from near to far  $\tau$ 's and  $\pi$ 's as the main components of the events. Again, the best discriminant is the  $[\pi\pi]$  distribution. This reflects the  $R$ -dominated character of  $\tilde{\tau}$  as opposed to the  $L$  current coupled to the Kaluza-Klein state  $Z_1 \simeq W^3$  [16].

Experimental analyses of  $\tau$  particles are a difficult task at LHC. Isolation criteria of hadron and lepton tracks must be met which reduce the efficiencies strongly for small transverse momenta.<sup>‡</sup> Stringent transverse momentum cuts increase the efficiencies but reduce the primary event number and erase the difference between  $R$  and  $L$  distributions. On the other hand, fairly small transverse momentum cuts reduce the efficiencies but do not reduce the primary event number and the  $R/L$  sensitivity of the

<sup>‡</sup>We are very grateful for comments on these problems by K. Desch, D. Mangeol and J. Mnich.

distributions. Optimization procedures in this context are far beyond the scope of this theoretical note. Experimental details may be studied in the recent reports [2,17] in which the analysis of di- $\tau$  final states is presented for supersymmetry cascades of type (1) at LHC.

In Fig. 4(a) it is shown how a cut of 15 GeV on the pion transverse momenta modifies the SUSY and UED' distributions of the  $\pi\pi$  invariant mass. Given the specific SPS1a mass differences, the SUSY  $LR$ -dominated distribution is mildly affected while the UED'  $LL$ -dominated distribution is shifted more strongly. [The different size of the shifts can be traced back to the different shapes of the  $R$  and  $L$  fragmentation functions. Since  $L$  fragmentation is soft, more events with low transverse momentum are removed by the cut and the shift is correspondingly larger than for hard  $R$  fragmentation.] Apparently, the transverse momentum cut does not erase the distinctive difference between the  $LR$  and  $LL$  distributions.

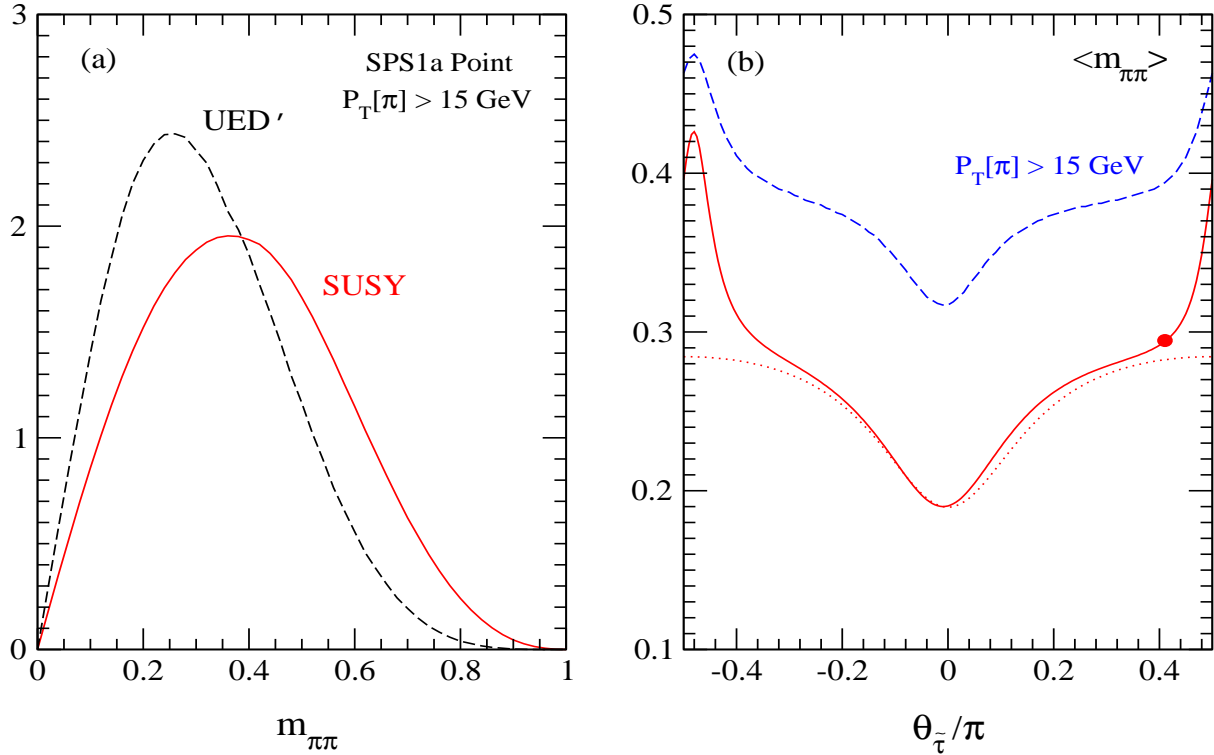


**Figure 4:** (a) The SUSY and UED' distributions of the  $\pi\pi$  invariant mass with a cut of 15 GeV on the pion transverse momenta; and (b) the dependence of the expectation value  $\langle m_{\pi\pi} \rangle$  on the stau mixing angle  $\theta_{\tilde{\tau}}$  [in units of  $\pi$ ] for the SPS1a values of  $\tan\beta, M_{1,2}, \mu$  and the lighter stau mass  $m_{\tilde{\tau}_1}$  [without (red) and with (blue)  $\pi$  transverse momentum cut]. The (red) dot on the solid line denotes the value of  $\langle m_{\pi\pi} \rangle$  at the SPS1a point. The (red) dotted line represents the average values of  $\langle m_{\pi\pi} \rangle$  if  $\tilde{\chi}_{1,2}^0$  are unmixed pure bino-like and wino-like states, respectively.



4.) Finally we study the dependence of the  $[\pi\pi]$  distribution on the stau mixing angle  $\theta_{\tilde{\tau}}$ , setting all other parameters to their SPS1a values:

$$\tilde{\tau}_1 = \cos\theta_{\tilde{\tau}}\tilde{\tau}_L + \sin\theta_{\tilde{\tau}}\tilde{\tau}_R \quad (22)$$

$$\tilde{\tau}_2 = -\sin\theta_{\tilde{\tau}}\tilde{\tau}_L + \cos\theta_{\tilde{\tau}}\tilde{\tau}_R \quad (23)$$

The expectation value of the  $\pi\pi$  mass distribution is given in terms of the  $\tau\tilde{\tau}\tilde{\chi}$  vertices in Eqs. (9) and (10) by

$$\langle m_{\pi\pi} \rangle = \frac{32}{675} (9\omega_{2R}\omega_{1R} + 6\omega_{2R}\omega_{1L} + 6\omega_{2L}\omega_{1R} + 4\omega_{2L}\omega_{1L}) \quad (24)$$

$$\omega_{j\alpha} = \frac{|A_{\alpha 1j}^\tau|^2}{|A_{R1j}^\tau|^2 + |A_{L1j}^\tau|^2} \quad [j = 1, 2; \alpha = R, L] \quad (25)$$

The coefficients are products of the average  $\tau\tau$  invariant mass and the average momenta in the  $\tau \rightarrow \pi$  fragmentations. The predictions for the  $[\pi\pi]$  invariant-mass expectation value are shown in Fig. 4(b). The effect of a 15 GeV cut on the transverse momenta of the pions is included for comparison. The stau mixing angle of the SPS1a point,  $\theta_{\tilde{\tau}} \approx 0.4\pi$ , is indicated by the red dot in the figure, representing a state  $\tilde{\tau}_1$  with 90%  $\tilde{\tau}_R$  and 10%  $\tilde{\tau}_L$  components. The large sensitivity of the  $[\pi\pi]$  invariant mass to the mixing angle can be traced back to the fact that the neutralino  $\tilde{\chi}_2^0$  is nearly wino-like ( $N_{22} = -0.94$ ). For  $\theta_{\tilde{\tau}} = \pm\pi/2$  the  $R$  state  $\tilde{\tau}_1 = \tilde{\tau}_R$ , couples to  $\tilde{\chi}_2^0$  only through its small higgsino and U(1) gaugino components (*i.e.*  $h_\tau N_{23} = 0.04$  and  $N_{21} = -0.11$ ). However, once the mixing angle deviates slightly from  $\pm\pi/2$  the “near” tau lepton  $\tau_n$  coupling quickly becomes  $L$ -dominated, *cf.* Eqs. (9/10), reducing  $\omega_{RR}$  and  $\omega_{RL}$  drastically and increasing  $\omega_{LR}$  significantly. [The sharp increase near the left edge is due to the constructive interference between the U(1) gaugino and higgsino contributions to the coupling  $A_{R12}^\tau$ .] The cut on the pion transverse momenta modifies the  $m_{\pi\pi}$  distribution, moderately for  $R$  chirality and strongly for  $L$  chirality. Nevertheless, for each chirality combination the shift is predicted completely in terms of the squark,  $\tilde{\chi}_{1,2}^0$  and  $\tilde{\tau}_1$  masses, and the shapes of the  $R/L$  fragmentation functions, so that it is under proper control. In particular, the relatively large increase of the average  $\langle m_{\pi\pi} \rangle$  near  $\theta_{\tilde{\tau}} = 0$  compared with  $\pm\pi/2$  follows from the large effect of the transverse momentum cut due to the soft  $L$  fragmentation, *cf.* Fig. 4(b).

5.) *In summary.* The analysis of  $\tau$  polarization in cascade decays provides valuable information on chirality-type and mixing of supersymmetric particles. The most exciting effects are predicted for the invariant mass distributions in the  $\pi\pi$  sector generated by the two polarized  $\tau$  decays. This is strikingly different from the lepton-lepton invariant mass distributions in the first two generations which do not depend on the  $R$  and  $L$  couplings. It is particularly important to notice that these polarization effects are independent of the couplings in the squark/quark sector and also of the polarization state of the parent  $\tilde{\chi}_2^0$  generating the final  $\tau\tau\tilde{\chi}_1^0$  state.

## Acknowledgments

Communications on experimental aspects of  $\tau$  identification from K. Desch, D. Mangeol and J. Mnich are gratefully acknowledged. Also discussions with M. Nojiri have been of great help. The work was supported in part by the Grant-in-Aid for Scientific Research (No. 17540281) from the Japan Ministry of Education, Culture, Sports, Science, and Technology. It was also supported in part by the Korea Research Foundation Grant (KRF-2006-013-C00097), by KOSEF through CHEP at Kyungpook National University and by Deutsche Forschungsgemeinschaft. S.Y.C. is grateful for support during his visit to DESY. P.M.Z. thanks for the warm hospitality extended to him by the KEK Theory Group.

## References

- [1] ATLAS Technical Proposal, CERN-LHCC-94-43.
- [2] CMS Physics, Technical Design Report, CERN-LHCC-2006-021.
- [3] W. Beenakker, R. Hopker, M. Spira and P. M. Zerwas, Nucl. Phys. B **492** (1997) 51 [hep-ph/9610490].
- [4] H. Bachacou, I. Hinchliffe and F. E. Paige, Phys. Rev. D **62** (2000) 015009 [hep-ph/9907518].
- [5] B. C. Allanach *et al.*, Eur. Phys. J. C **25** (2002) 113 [hep-ph/0202233].
- [6] G. Weiglein *et al.* [LHC/LC Study Group], Phys. Rept. **426** (2006) 47 [hep-ph/0410364].
- [7] A. J. Barr, Phys. Lett. B **596**, 205 (2004) [hep-ph/0405052].
- [8] T. Goto, K. Kawagoe and M. M. Nojiri, Phys. Rev. D **70** (2004) 075016 [Erratum-ibid. D **71** (2005) 059902] [hep-ph/0406317].
- [9] J. M. Smillie and B. R. Webber, JHEP **0510** (2005) 069 [hep-ph/0507170]; C. Athanasiou, C. G. Lester, J. M. Smillie and B. R. Webber, JHEP **0608** (2006) 055 [hep-ph/0605286].
- [10] L. T. Wang and I. Yavin, arXiv:hep-ph/0605296.
- [11] M. M. Nojiri, Phys. Rev. D **51** (1995) 6281 [hep-ph/9412374]; M. M. Nojiri, K. Fujii and T. Tsukamoto, Phys. Rev. D **54** (1996) 6756 [hep-ph/9606370].
- [12] B. K. Bullock, K. Hagiwara and A. D. Martin, Nucl. Phys. B **395** (1993) 499.

- [13] S. Y. Choi, J. Kalinowski, G. A. Moortgat-Pick and P. M. Zerwas, Eur. Phys. J. C **22** (2001) 563 [Addendum-ibid. C **23** (2002) 769] [hep-ph/0108117].
- [14] E. Boos, H. U. Martyn, G. A. Moortgat-Pick, M. Sachwitz, A. Sherstnev and P. M. Zerwas, Eur. Phys. J. C **30**, 395 (2003) [hep-ph/0303110].
- [15] T. Appelquist, H. C. Cheng and B. A. Dobrescu, Phys. Rev. D **64**, 035002 (2001) [hep-ph/0012100].
- [16] H. C. Cheng, K. T. Matchev and M. Schmaltz, Phys. Rev. D **66** (2002) 036005 [hep-ph/0204342].
- [17] D. J. Mangeol and U. Goerlach, *Search for  $\tilde{\chi}_2^0$  decays to  $\tilde{\tau}\tau$  and SUSY mass spectrum measurement using  $di\text{-}\tau$  final states*, CMS note 2006/096.